**New Folder Name** High Sensitivity Antenna

LIGO-T930015-00-D

# High Sensitivity Gravitational Wave Antenna with Parametric Transducer Readout

D. G. Blair, E. N. Ivanov, M. E. Tobar, P. J. Turner, F. van Kann
Physics Department, University of Western Australia, Nedlands, WA, 6009

A high-Q niobium resonant mass gravitational radiation antenna with a superconducting parametric transducer is shown to achieve a noise temperature of about 3 mK using a zero order predictor filter. This corresponds to a dimensionless strain sensitivity $h \sim 9\times10^{-19}$ for millisecond gravitational wave bursts. The predicted intrinsic cold damping of a parametric transducer is confirmed, along with predicted back-action limits on the sensitivity. While the antenna has the highest intrinsic Q-factor and lowest noise temperature ever observed in a full scale antenna, the possibility of further improvements is demonstrated.

PACS numbers: 04.80. +z, 06.70. Dn

Resonant mass gravitational wave antennas have been painstakingly improved over the past 20 years [1,2]. Cryogenic operation, superconducting transducers, improved vibration isolation and increased acoustic Q-factors have contributed to a $10^4$ fold improvement in energy sensitivity over Weber's original antennas [3]. Two types of superconducting transducers have been developed: SQUID based inductive or capacitive sensors [4] and parametric transducers utilizing radio frequency[5] or microwave resonators [6]. Although the latter devices have been promoted as potentially very sensitive transducers, they have not previously been successfully implemented in a full scale antenna. The problems encountered included the possibility of the transducer parametricly exciting the antenna [7], excess noise due to the microwave readout electronics, and the effects of low frequency seismic noise.

In this letter we report the first successful operation of a large scale cryogenic resonant mass antenna instrumented with a superconducting parametric transducer. Parametric instability of the antenna is avoided by controlled operation in the cold damped regime where the mean energy of antenna displacement fluctuations is about 10 times less than the equilibrium value. The noise in the readout electronics is reduced by using a 10 GHz sapphire loaded superconducting cavity oscillator [8] with the lowest ever measured phase noise at 1 kHz [9], and cryogenic low-noise microwave amplification employing an active carrier suppression technique [10]. The effect of seismic noise is greatly reduced by an improved cryogenic vibration isolation system [11] and a non-contacting microwave coupling to the transducer [12].

Figure 1 shows a simplified diagram of the antenna. The antenna operates at about 5 K, and consists of a 1.5 tonne Nb bar with a fundamental frequency of 710 Hz bonded to a 0.5 kg Nb bending flap with a resonant frequency of 700 Hz. The observed coupled frequencies are at 713 Hz (bar-like mode) and 694 Hz (flap-like mode). The bending flap acts as a mechanical amplifier of the bar motion so the antenna may be better sensed above the transducer noise [13].

The vibrational state of antenna is continuously monitored by a superconducting re-entrant cavity whose capacitance is modulated by the motion of the antenna. The low-noise microwave pump signal is coupled radiatively to the transducer by two miniature microstrip antennas [11]. These eliminate the need for any wiring connection between the antenna and readout system, allowing a high degree of mechanical isolation of the antenna from the environment. The signal from the transducer is processed in a phase sensitive microwave signal processing circuit (MSPC), comprising an active carrier suppression interferometer, a cryogenic amplifier, and a room temperature mixer. The carrier suppression interferometer is a key element of the MSPC which allows a low-noise cryogenic amplification of the extremely weak signal reflected from the transducer. Two servo control systems provide stable operation of the MSPC. The first servo maintains a constant negative offset between the pump source and transducer resonant frequency. This is required to maintain parametric cold damping (see below), and it also suppresses variations of the transducer resonant frequency caused by low frequency seismic excitation of the normal modes in the vibration isolation system. The second servo maintains the carrier suppression interferometer locked to the "dark fringe" despite the low frequency rocking motions of the bar.

The interaction of the parametric transducer and the antenna causes changes in the resonant frequency and in the Q-factor of the antenna normal modes [14,15]. Experimental observations of this effect are shown in Figure 2a. The unperturbed Q-factors measured at a very low microwave power in the input of the transducer, $P_{in}$=-45 dBm, are equal to $3*10^7$ and $1.3*10^7$ for the bar-like mode (713 Hz) and the flap-like mode (694 Hz) respectively. The energy of the displacement fluctuations of the flap at the frequencies of the normal modes can be expressed in terms of a mode temperature, $T_m$. At $P_{in}$=-45 dBm, $T_m$ is equal (within experimental error) to the physical temperature of the antenna (about 5 K), consistent with the expected Brownian motion in the antenna.

Increasing the microwave power reduces both the Q-factor and the mode temperature. The damping is non dissipative and preserves the ratio $T_m/Q$, confirming the intrinsic cold damped operation of the transducer. In this regime the overall performance of the antenna improves with increased input power $P_{in}$. However at an input power of -12 dBm a point occurs in the $T_m/Q$ versus $P_{in}$ relation (see fig. 2b), at which the back-action noise is equal to the thermal noise. Above this power back-action noise dominates, increasing the energy of antenna vibration above the level determined by the Brownian motion. This noise is caused by amplitude fluctuations of the pump which produces fluctuations in the attractive force acting between the transducer and antenna. Back-action noise is proportional to the input power squared and reduces the antenna sensitivity at high levels of $P_{in}$.

For measuring the antenna noise temperature, $T_n$, a zero order prediction (ZOP) algorithm based on the two channel synchronous detection system has been implemented[16]. When properly tuned this algorithm achieves a signal-to-noise ratio only 2.3 times less than an ideal optimal filter. The noise temperature is determined by fitting the observed energy distribution of the voltage noise at the filter output to a Boltzmann distribution. The conversion from displacement to electrical units is determined from the known transducer tuning coefficient df/dx and the measured transducer Q-factor. A reproducible exponential behaviour is achieved, with a low level of excess high energy events.

Noise temperature measurements for the 713 Hz mode versus sampling time are shown in Figure 3. A minimum in $T_n$ occurs when contributions from the narrow band noise (Brownian motion and back-action noise) and the broad band noise (additive noise of the readout electronics) are equal. The antenna bandwidth $\Delta f$ is the reciprocal of the sampling time at which the minimum of $T_n$ is achieved. At $P_{in}$=-5 dBm the minimum $T_n$ is 10 mK and $\Delta f$ is 3 Hz (curve 1). At a lower power, -10 dBm, $T_n$=4 mK has been measured for the 713 Hz mode, but $\Delta f$ is reduced to 1 Hz (curve 2). To calculate the overall noise temperature of the antenna the flap like mode must also be taken into account, using the relation $1/T_n=1/T_{n(713)}+1/T_{n(694)}$. This gives a detector noise temperature of 3mK. Thus with our present scheme we expect the antenna to operate at a noise temperature of about 1mK when the optimal filter is implemented. This result is consistent with a detailed mathematical model of the detector [17].

From curve 2 in figure 3 the bandwidth of our antenna is about 1 Hz, which is less than optimum because the bar and flap are detuned by 10 Hz. This is consistent with our model, which also predicts that more accurate tuning would improve the bandwidth by up to a factor of 3. However, such detuning effects the strain sensitivity only to second order and would remain unchanged. Electronic tuning can be achieved by exploiting the parametric interactions of the transducer with the bending flap, but only if the flap mode frequency is above the bar frequency (which is not the present case) [13]. To increase the bandwidth and sensitivity for the existing antenna configuration, both series and back action noise must be reduced. Both noise sources are believed to be due to amplitude noise in the pump oscillator. Power stabilisation schemes are expected to reduce the a.m. noise from -140 to -160 dBc/Hz, and the series noise from $5\times10^{-17}$ to $1.5\times10^{-18}$ $m/\sqrt{Hz}$. The model shows that for $P_{in}$=-3 dBm, the noise temperature is reduced to 30 $\mu$K, corresponding to a 1ms burst strain sensitivity of $10^{-19}$ with a bandwidth of about 10 Hz. If the bar and the flap were tuned properly the bandwidth would be increased to about 20 Hz. Except for the tuning, these improvements can be implemented without interrupting long term operation. The antenna will now be prepared to operate for extended periods in coincidence with the cryogenic Al bars of the LSU and Rome groups.

We would like to thank Dr. A. G. Mann, Dr. P. J. Veitch, Dr. N. P. Linthorne and Mr. Ik Siong Heng for their contribution towards the success of this experiment, and Dr. C. Edwards and Prof M.J. Buckingham for their long term support. This work would have been impossible without the outstanding contributions of our workshop staff and was supported by Australian Research Council.

## References

1. W.O. Hamilton, in *Proc. of the Sixth Marcel Grossmann Meeting on General Relativity* (World Scientific, Singapore, 1992) pp. 988.

2. P. Astone et al, in Gravitational Astronomy: Instrument Design and Astrophysical Prospects, edited by D.E. McClelland and H.A. Bachor (World Scientific, Singapore, 1991) pp. 189.

3. J. Weber, Phys. Rev., 117, pp. 306, (1960)

4. P.F. Michelson and R. C. Taber, J. Appl. Phys. 52, pp. 4313 (1981)

5. M.F. Bocko and W.W. Johnson, Phys. Rev. A, 30(4), pp. 2135 (1984)

6. P.J. Veitch, D.G. Blair, N.P. Linthorne, L.D. Mann and D.K. Ramm, Rev. Sci. Instrum., 58(10) pp. (1987)

7. V. B. Braginsky and A. B. Manukin, in *Measurement of Weak Forces in Physics Experiments* (Chicago, University of Chicago Press, 1977), p. 19

8. A. J. Giles, S. K. Jones, D.G. Blair and M. J. Buckingham in Proc. 43rd Annual Symp. of Freq. Control, pp. 89 (1989)

9. M.E. Tobar and D.G. Blair, IEEE MTT. Trans., 42(2) (1994)

10. E. N. Ivanov, P. J. Turner and D. G. Blair accepted for publication in Review of Scientific Instruments, August 1993.

11. D.G. Blair et al, in *Some New Trends on Fluid Mechanics and Theoretical Physics*, edited by C.C. Lin and Ning Hu (Peking University Press, Beijing, 1993) pp. 591.

12. E. N. Ivanov, M. E. Tobar, P. J. Turner and D. G. Blair, Review of Scientific Instruments, 64 (7), 1993, p. 1905.

13. H.J. Paik, Ph.D. Thesis, Stanford University (1974)

14. N.P. Linthorne, P.J. Veitch and D.G. Blair, J. Phys D, 23, pp. 1, (1990)

15. M. E. Tobar and D. G. Blair, J. Phys. D: Appl. Phys., 26, pp. 2276 (1993)

16. G. V. Pallottino and G. Pizella, in*Detection of Gravitational Waves*, edited by D. G. Blair (Cambridge University Press, Cambridge, 1991), p. 242

17. M.E. Tobar and D.G. Blair, submitted to Rev. of Sci. Instrum., 1993.

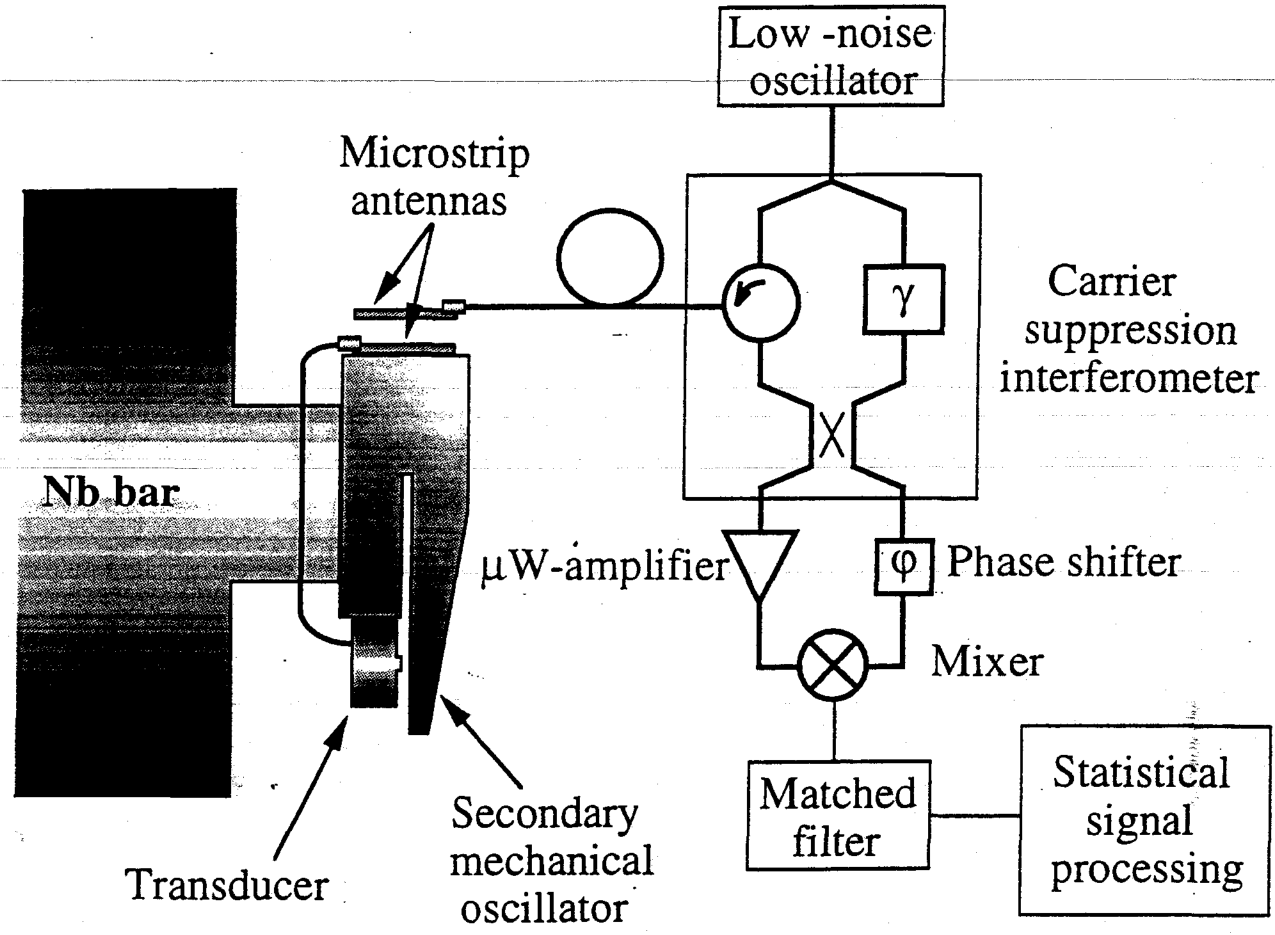

Low -noise oscillator
Microstrip antennas
Carrier suppression interferometer
γ
Nb bar
μW-amplifier
φ
Phase shifter
Mixer
Matched filter
Statistical signal processing
Transducer
Secondary mechanical oscillator

Fig. 1

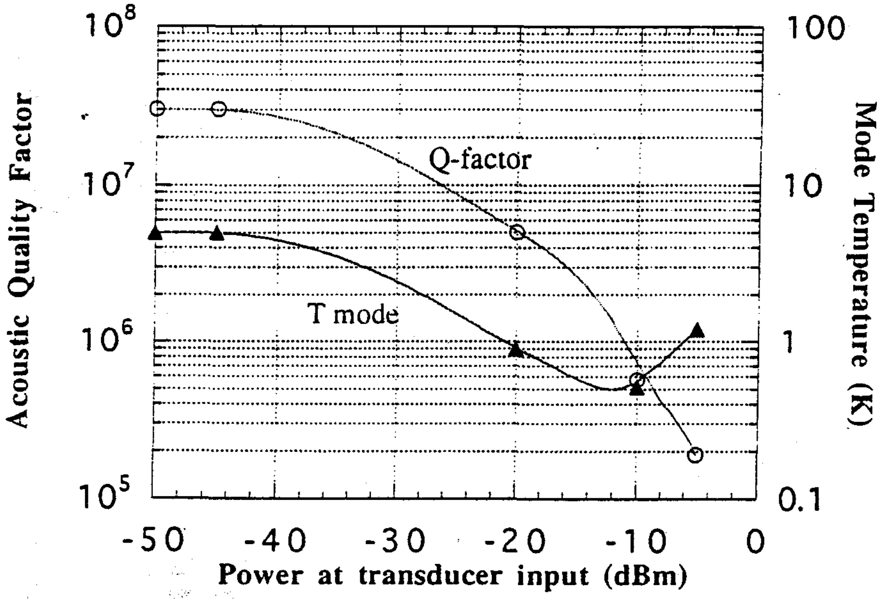

$10^8$
$10^7$
$10^6$
$10^5$
Acoustic Quality Factor
100
10
1
0.1
Mode Temperature (K)
Q-factor
T mode
-50
-40
-30
-20
-10
0
Power at transducer input (dBm)

Fig 2a

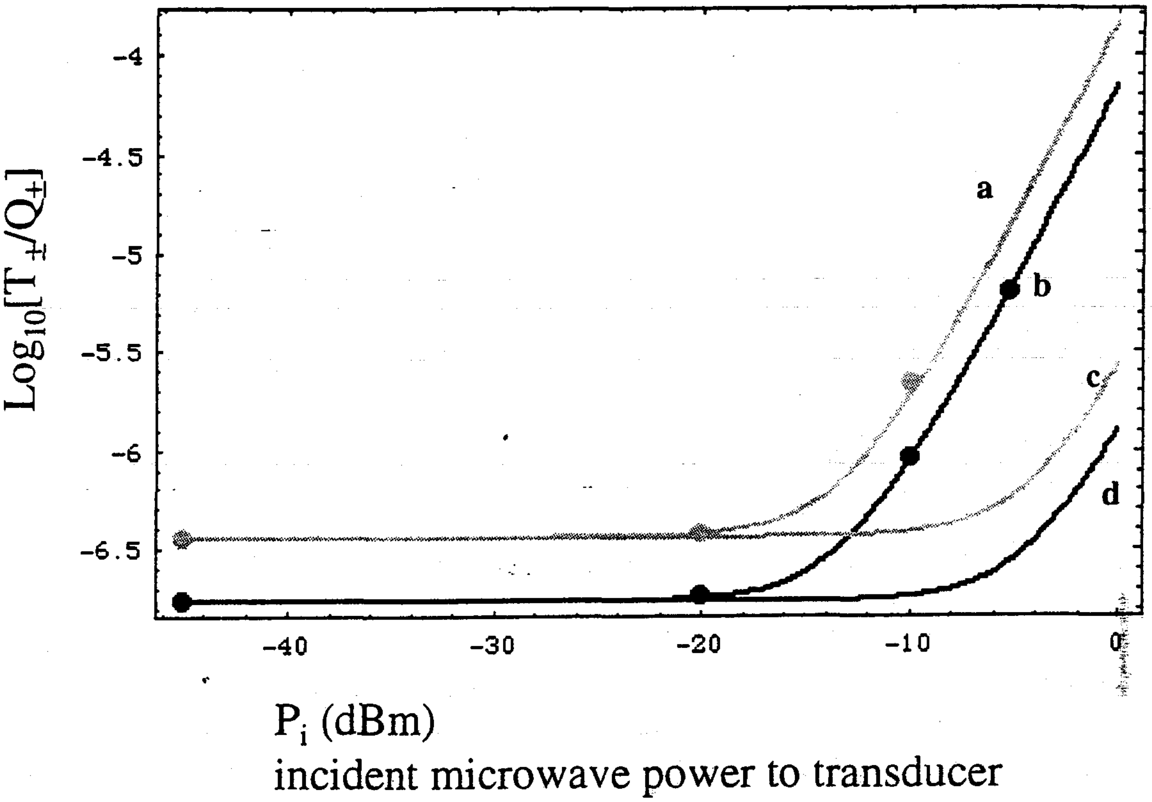
-4
-4.5
-5
-5.5
-6
-6.5
$\mathrm{Log}_{10}[T_\pm/Q_\pm]$
a
b
c
d
-40
-30
-20
-10
0
$P_i$ (dBm)
incident microwave power to transducer

Figure 2b

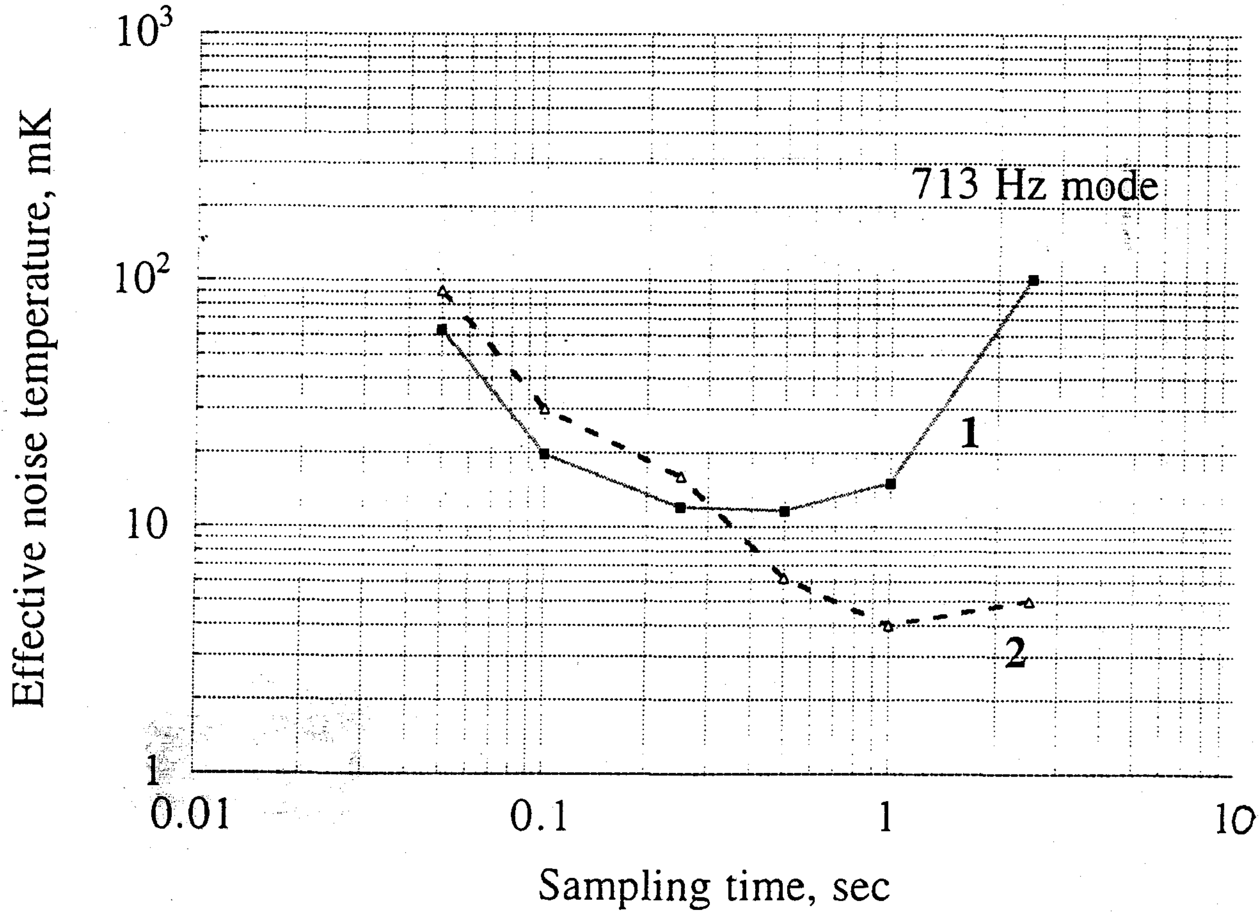

$10^3$
$10^2$
10
1
0.01
0.1
1
10
Effective noise temperature, mK
Sampling time, sec
713 Hz mode
1
2

Fig 3